

Low and High Energy Phenomenology of Quark-Lepton Complementary Scenarios

Kathrin A. Hochmuth^{a*} and Werner Rodejohann^{b†}

^a*Max-Planck-Institut für Physik (Werner-Heisenberg-Institut),
Föhringer Ring 6, D-80805 München, Germany*

^b*Physik-Department, Technische Universität München,
James-Frank-Strasse, D-85748 Garching, Germany*

Abstract

We conduct a detailed analysis of the phenomenology of two predictive see-saw scenarios leading to Quark-Lepton Complementary. In both cases we discuss the neutrino mixing observables and their correlations, neutrinoless double beta decay and lepton flavor violating decays such as $\mu \rightarrow e\gamma$. We also comment on leptogenesis. The first scenario is disfavored on the level of one to two standard deviations, in particular due to its prediction for $|U_{e3}|$. Moreover, there can only be leptogenesis in highly fine-tuned situations, one of which corresponds to quasi-degenerate light neutrinos and sizable cancellations in neutrinoless double beta decay. The decays $\mu \rightarrow e\gamma$ and $\tau \rightarrow \mu\gamma$ are typically observable unless the SUSY masses approach the TeV scale. In the second scenario leptogenesis is impossible. It is however in perfect agreement with all oscillation data. The prediction for $\mu \rightarrow e\gamma$ is in general too large, unless the SUSY masses are in the range of several TeV. In this case $\tau \rightarrow e\gamma$ and $\tau \rightarrow \mu\gamma$ are unobservable.

*email: hochmuth@mppmu.mpg.de

†email: werner_odejohann@ph.tum.de

1 Introduction

The neutrino mass and mixing phenomena [1] have provided us with some exciting hints towards the structure of the underlying theory of flavor. In particular, based on observations implying that the CKM and PMNS matrices are linked by a profound connection, an interesting class of models arises. The CKM matrix is to zeroth order the unit matrix plus a small correction, given by the sine of the Cabibbo angle, $\sin\theta_C = 0.23$. Hence, in the quark sector mixing is absent at zeroth order and the deviation from *no mixing* is small. To make a connection to the lepton sector, it was noted [2] that the deviation from *maximal mixing* is small. Indeed, using the bimaximal [3] mixing scenario as the zeroth order scheme and interpreting the observed deviation from maximal solar neutrino mixing as a small expansion parameter, one can write [2]:

$$|U_{e2}| \equiv \sqrt{\frac{1}{2}} (1 - \lambda_\nu) . \quad (1)$$

With current experimental information [4], we obtain $\lambda_\nu = 0.21_{-0.03, 0.07, 0.11}^{+0.04, 0.08, 0.11}$, where we have inserted the best-fit values and the 1, 2 and 3σ ranges of the relevant oscillation parameters. This number is remarkably similar to the Cabibbo angle [2]. In fact, the so called QLC-relation (Quark-Lepton Complementary) [5, 6]

$$\theta_{12} + \theta_C = \frac{\pi}{4} \quad (2)$$

has been suggested and several situations in which it can be realized have been discussed [5, 6, 7, 8, 9]. In general, the PMNS matrix is given by $U_\ell^\dagger U_\nu$, where U_ν diagonalizes the neutrino mass matrix and U_ℓ originates from the charged lepton diagonalization. Apparently, deviations from maximal θ_{12} as implied by Eqs. (1, 2) can be obtained if the neutrino mass matrix corresponds to bimaximal mixing and the charged lepton mass matrix is diagonalized by either the CKM or a CKM-like [10, 11] matrix. The opposite case, namely bimaximal mixing from the charged lepton sector and a CKM correction from the neutrinos, can also be realized, which indicates two possibilities for the approximate realization of Eq. (2).

In the present article we fully analyze the phenomenology of these two popular scenarios, proposed in [5, 6], leading to an approximate realization of QLC within the see-saw mechanism [12]. The two scenarios show the feature that the matrix perturbing the bimaximal mixing scenario is exactly the CKM matrix and not just a CKM-like matrix, which minimizes the number of free parameters. We study the neutrino oscillation phenomenology, neutrinoless double beta decay and – in context of the see-saw mechanism – lepton flavor violating decays such as $\mu \rightarrow e\gamma$. We present our results of the correlations between the observables in several plots. In contrast to many previous works, we include the full number of possible CP phases. This is a new approach particularly for the second scenario, where bimaximal mixing arises from the charged lepton sector. For both scenarios we comment on the prospects of leptogenesis. We begin in Sec. 2 with an introduction to the formalism

required to study the observables. In Secs. 3 and 4 we discuss the phenomenology of the two scenarios, before we conclude in Sec. 5 with a summary of our results.

2 Formalism

In this section we briefly introduce the required formalism to analyze the QLC scenarios. First, we discuss lepton and quark mixing before turning to lepton flavor violation, whose connection to low energy neutrino physics is implied by the see-saw mechanism. Conclusively, the principles of leptogenesis are outlined.

2.1 Neutrino Masses, Lepton- and Quark-Mixing

The two scenarios leading to QLC are set within the framework of the see-saw mechanism for neutrino mass generation [12]. In general, one has the Lagrangian

$$\mathcal{L} = \frac{1}{2} \overline{N_R} M_R N_R^c + \overline{\ell_R} m_\ell \ell_L + \overline{N_R} m_D \nu_L, \quad (3)$$

where N_R are the right-handed Majorana singlets, $\ell_{L,R}$ the left- and right-handed charged leptons and ν_L the left-handed neutrinos. The mass matrix of the charged leptons is m_ℓ , m_D is the Dirac neutrino mass matrix and M_R the heavy right-handed Majorana neutrino mass matrix. As $M_R \gg m_D$, Eq. (3) leads to an effective neutrino mass matrix at low energies, defined as

$$m_\nu = -m_D^T M_R^{-1} m_D = U_\nu^* m_\nu^{\text{diag}} U_\nu^\dagger, \quad (4)$$

where U_ν transforms m_ν to m_ν^{diag} , with the neutrino masses $m_{1,2,3}$ as diagonal entries. When diagonalizing the charged lepton mass matrix as $m_\ell = V_\ell m_\ell^{\text{diag}} U_\ell^\dagger$, we can rotate $\nu_L \rightarrow U_\nu^\dagger \nu_L$, $\ell_R \rightarrow V_\ell^\dagger \ell_R$ and $\ell_L \rightarrow U_\ell^\dagger \ell_L$. From the charged current term, which is proportional to $\overline{\ell_L} \gamma^\mu \nu_L$, we thus obtain the PMNS matrix

$$U = U_\ell^\dagger U_\nu, \quad (5)$$

which we parameterize as

$$U = \begin{pmatrix} c_{12}c_{13} & s_{12}c_{13} & s_{13}e^{-i\delta} \\ -s_{12}c_{23} - c_{12}s_{23}s_{13}e^{i\delta} & c_{12}c_{23} - s_{12}s_{23}s_{13}e^{i\delta} & s_{23}c_{13} \\ s_{12}s_{23} - c_{12}c_{23}s_{13}e^{i\delta} & -c_{12}s_{23} - s_{12}c_{23}s_{13}e^{i\delta} & c_{23}c_{13} \end{pmatrix} \text{diag}(1, e^{i\alpha}, e^{i(\beta+\delta)}), \quad (6)$$

where we have used the usual notations $c_{ij} = \cos \theta_{ij}$, $s_{ij} = \sin \theta_{ij}$. We have also introduced the Dirac CP -violating phase δ and the two Majorana CP -violating phases α and β [13]. The oscillation parameters can be expressed by two independent mass squared differences, $\Delta m_\odot^2 = m_2^2 - m_1^2$ and $\Delta m_\text{A}^2 = |m_3^2 - m_1^2|$, as well as three mixing angles, whose exact values

are a matter of intense research projects [1]. Their current best-fit values and their 1, 2 and 3σ ranges are according to [4]:

$$\begin{aligned}
\Delta m_{\odot}^2 &= (7.9_{-0.3, 0.6, 0.8}^{+0.3, 0.6, 1.0}) \cdot 10^{-5} \text{ eV}^2 , \\
\sin^2 \theta_{12} &= 0.31_{-0.03, 0.05, 0.07}^{+0.02, 0.06, 0.09} , \\
\Delta m_{\text{A}}^2 &= (2.2_{-0.27, 0.5, 0.8}^{+0.37, 0.7, 1.1}) \cdot 10^{-3} \text{ eV}^2 , \\
\sin^2 \theta_{23} &= 0.50_{-0.05, 0.12, 0.16}^{+0.06, 0.14, 0.18} , \\
\sin^2 \theta_{13} &< 0.012 (0.028, 0.046) .
\end{aligned} \tag{7}$$

The present best-fit value for $\sin^2 \theta_{13}$ is 0.

Turning to the quark sector, the CKM matrix is [14]

$$V = \begin{pmatrix} 1 - \frac{1}{2} \lambda^2 & \lambda & A \lambda^3 (\rho - i\eta) \\ -\lambda & 1 - \frac{1}{2} \lambda^2 & A \lambda^2 \\ A \lambda^3 (1 - \rho + i\eta) & -A \lambda^2 & 1 \end{pmatrix} + \mathcal{O}(\lambda^4) . \tag{8}$$

In analogy to the PMNS matrix it is a product of two unitary matrices, $V = V_{\text{up}}^\dagger V_{\text{down}}$, where V_{up} (V_{down}) diagonalizes the up-(down-)quark mass matrix. As reported in [15] the best-fit values as well as the 1, 2 and 3σ ranges of the parameters λ , A , $\bar{\rho}$, $\bar{\eta}$ are

$$\begin{aligned}
\lambda = \sin \theta_C &= 0.2272_{-0.0010, 0.0020, 0.0030}^{+0.0010, 0.0020, 0.0030} , \\
A &= 0.809_{-0.014, 0.028, 0.042}^{+0.014, 0.029, 0.044} , \\
\bar{\rho} &= 0.197_{-0.030, 0.087, 0.133}^{+0.026, 0.050, 0.074} , \\
\bar{\eta} &= 0.339_{-0.018, 0.037, 0.057}^{+0.019, 0.047, 0.075} ,
\end{aligned} \tag{9}$$

where $\bar{\rho} = \rho(1 - \lambda^2/2)$ and $\bar{\eta} = \eta(1 - \lambda^2/2)$. Effects caused by CP violation are always proportional to a Jarlskog invariant [16], defined as

$$J_{CP} = -\text{Im}\{V_{ud} V_{cs} V_{us}^* V_{cd}^*\} \simeq A^2 \lambda^6 \bar{\eta} = (3.1_{-0.37, 0.74, 0.96}^{+0.43, 0.82, 1.08}) \cdot 10^{-5} . \tag{10}$$

The leptonic analogue of Eq. (10) is

$$J_{CP}^{\text{lep}} = \text{Im}\{U_{e1} U_{\mu 2} U_{e2}^* U_{\mu 1}^*\} = \frac{1}{8} \sin 2\theta_{12} \sin 2\theta_{23} \sin 2\theta_{13} \cos \theta_{13} \sin \delta , \tag{11}$$

where we have also given the explicit form of J_{CP}^{lep} with the parametrization of Eq. (6). There are two additional invariants, S_1 and S_2 [17], related to the Majorana phases:

$$S_1 = \text{Im}\{U_{e1} U_{e3}^*\} \text{ and } S_2 = \text{Im}\{U_{e2} U_{e3}^*\} , \tag{12}$$

which have no analogue in the quark sector.

2.2 Lepton Flavor Violation

The see-saw mechanism explains the smallness of neutrino masses, but due to the extreme heaviness of the right-handed Majorana neutrinos a direct test is not only challenging, but presumably impossible. Nonetheless a reconstruction of the see-saw parameter space is possible in supersymmetric (SUSY) scenarios. While being extremely suppressed when mediated by light neutrinos [18], Lepton Flavor Violating (LFV) decays such as $\mu \rightarrow e\gamma$ depend in the context of SUSY see-saw on the very same parameters responsible for neutrino masses and can be observable in this case [19]. The size and relative magnitudes of the decays are known to be a useful tool to distinguish between different models. In this work we will focus on models where SUSY is broken by gravity mediation, so called mSUGRA models. In this case there are four relevant parameters, which are defined at the GUT scale M_X , namely the universal scalar mass m_0 , the universal gaugino mass $m_{1/2}$, the universal trilinear coupling parameter A_0 and $\tan\beta$, which is the ratio of the vacuum expectation values of the up- and down-like Higgs doublets. For the branching ratios of the decays $\mu \rightarrow e\gamma$, $\tau \rightarrow e\gamma$ and $\tau \rightarrow \mu\gamma$ one can obtain in the leading-log approximation [19]

$$\text{BR}(l_i \rightarrow l_j \gamma) \simeq \frac{\Gamma(l_i \rightarrow e\nu\bar{\nu})}{\Gamma_{\text{total}}(l_i)} \frac{\alpha_{\text{em}}^3}{G_F^2 m_S^8 v_u^4} \left(\frac{(3m_0^2 + A_0^2)}{8\pi^2} \right)^2 \left| \left(\tilde{m}_D^\dagger L \tilde{m}_D \right)_{ij} \right|^2 \tan^2 \beta. \quad (13)$$

Here $v_u = v \sin\beta$ with $v = 174$ GeV, m_S represents a SUSY particle mass and $L = \delta_{ij} \ln M_X/M_i$, with M_i the heavy Majorana masses and $M_X = 2 \cdot 10^{16}$ GeV. Note that the formulae relevant for lepton flavor violation and leptogenesis have to be evaluated in the basis in which the charged leptons and the heavy Majorana neutrinos are real and diagonal. In this very basis we have to replace

$$m_D \rightarrow \tilde{m}_D = V_R^T m_D U_\ell, \quad (14)$$

where V_R diagonalizes the heavy Majorana mass matrix via $M_R = V_R^* M_R^{\text{diag}} V_R^\dagger$. The current limit on the branching ratio of $\mu \rightarrow e\gamma$ is $1.2 \cdot 10^{-11}$ at 90% C.L. [20]. A future improvement of two orders of magnitude is expected [21]. In most parts of the relevant soft SUSY breaking parameter space, the expression

$$m_S^8 \simeq 0.5 m_0^2 m_{1/2}^2 (m_0^2 + 0.6 m_{1/2}^2)^2, \quad (15)$$

is an excellent approximation to the results obtained in a full renormalization group analysis [22]. In order to simplify comparisons of different scenarios, it can be convenient to use “benchmark values” of the SUSY parameters. We choose both pints and slopes of the SPS values [23] displayed in Table 1.

In this context it might be worth commenting on renormalization aspects of the QLC relation (see also [6]). The running of the CKM parameters can always be neglected. However, the case of a large $\tan\beta \gtrsim 10$ in the MSSM can imprint sizeable effects on the neutrino observables, if the neutrino masses are not normally ordered. In our analysis, this would

| Point | m_0 | $m_{1/2}$ | A_0 | $\tan \beta$ |
|-------|-------|-----------|-------|--------------|
| 1a | 100 | 250 | -100 | 10 |
| 1b | 200 | 400 | 0 | 30 |
| 2 | 1450 | 300 | 0 | 10 |
| 3 | 90 | 400 | 0 | 10 |
| 4 | 400 | 300 | 0 | 50 |

Table 1: SPS Benchmark values for the mSUGRA parameters according to Ref. [23]. The values of m_0 , $m_{1/2}$ and A_0 are in GeV. The slope for Point 1a (2, 3) is $m_0 = -A_0 = 0.4 m_{1/2}$ ($m_0 = 2 m_{1/2} + 850$ GeV, $m_0 = \frac{1}{4} m_{1/2} - 10$ GeV) with varying $m_{1/2}$.

affect only the SPS point 4, when the neutrinos have an inverted hierarchy or are quasi-degenerate.

It proves useful to consider also the “double” ratios,

$$\begin{aligned}
R(21/31) &\equiv \frac{\text{BR}(\mu \rightarrow e + \gamma)}{\text{BR}(\tau \rightarrow e + \gamma)} \simeq \frac{\left| (\tilde{m}_D^\dagger L \tilde{m}_D)_{21} \right|^2}{\left| (\tilde{m}_D^\dagger L \tilde{m}_D)_{31} \right|^2}, \\
R(21/32) &\equiv \frac{\text{BR}(\mu \rightarrow e + \gamma)}{\text{BR}(\tau \rightarrow \mu + \gamma)} \simeq \frac{\left| (\tilde{m}_D^\dagger L \tilde{m}_D)_{21} \right|^2}{\left| (\tilde{m}_D^\dagger L \tilde{m}_D)_{32} \right|^2},
\end{aligned} \tag{16}$$

which are essentially independent on the SUSY parameters.

2.3 Leptogenesis

Since we will also comment on the possibility of leptogenesis in the QLC scenarios, we will summarize the key principles of this mechanism. An important challenge in modern cosmology is the explanation of the baryon asymmetry $\eta_B \simeq 6 \cdot 10^{-10}$ [25] of the Universe. One of the most popular mechanisms to create the baryon asymmetry is leptogenesis [26]. The heavy neutrinos, whose comparatively huge masses govern the smallness of the light neutrino masses, decay in the early Universe in Higgs bosons and leptons, thereby generating a lepton asymmetry, which in turn gets recycled into a baryon asymmetry via non-perturbative Standard Model processes. For recent reviews, see [27]. In principle, all three heavy neutrinos generate a decay asymmetry, which can be written as

$$\begin{aligned}
\varepsilon_i &= \frac{1}{8\pi v_u^2} \frac{1}{\left(\tilde{m}_D \tilde{m}_D^\dagger \right)_{ii}} \sum_{j \neq i} \text{Im} \left\{ \left(\tilde{m}_D \tilde{m}_D^\dagger \right)_{ji}^2 \right\} \sqrt{x_j} \left(\frac{2}{1-x_j} - \ln \left(\frac{1+x_j}{x_j} \right) \right), \\
\varepsilon_1 &\simeq -\frac{3}{8\pi v_u^2} \frac{1}{\left(\tilde{m}_D \tilde{m}_D^\dagger \right)_{11}} \sum_{j=2,3} \text{Im} \left\{ \left(\tilde{m}_D \tilde{m}_D^\dagger \right)_{j1}^2 \right\} \frac{M_1}{M_j},
\end{aligned} \tag{17}$$

where $x_j = M_j^2/M_i^2$. This is the general form of ε_i and the limit for ε_1 in case of $M_3 \gg M_2 \gg M_1$. Note that the decay asymmetries depend on $\tilde{m}_D \tilde{m}_D^\dagger$, which has to be compared to the dependence on $\tilde{m}_D^\dagger \tilde{m}_D$ governing the LFV decays. In the case $M_3 \gg M_2 \gg M_1$ only ε_1 plays a role, and dedicated numerical studies [27, 28] have shown that in case of the MSSM and a hierarchical spectrum of the heavy Majorana neutrino masses, successful thermal leptogenesis is only possible for

$$m_1 \lesssim 0.1 \text{ eV and } M_1 \gtrsim 10^9 \text{ GeV} . \quad (18)$$

However, it can occur in certain models that the lightest heavy neutrino mass is smaller than the limit of 10^9 GeV given above. We will encounter a scenario like this in the next section. There are two possible ways to resolve this problem:

- (i) a fine-tuned situation in which the heavy Majorana neutrinos are quasi-degenerate, as has been analyzed in [29];
- (ii) turning to non-thermal leptogenesis, i.e., the production of heavy neutrinos via inflaton decay [30].

The second possibility is a more model dependent case and complicates the situation, as the reheating temperature, the mass of the inflaton and the corresponding branching ratios for its decay into the Majorana neutrinos need to be known.

3 First Realization of QLC

The first framework in which our analysis is set is the following:

- we assume the conventional see-saw mechanism to generate the neutrino mass matrix $m_\nu = -m_D^T M_R^{-1} m_D$. Diagonalization of m_ν is achieved via $m_\nu = U_\nu^* m_\nu^{\text{diag}} U_\nu^\dagger$ and U_ν produces exact bimaximal mixing;
- the PMNS matrix is given by $U = U_\ell^\dagger U_\nu$, where U_ℓ corresponds to the CKM matrix V . This can be achieved in some $SU(5)$ models, in which $m_\ell = m_{\text{down}}^T$, where m_{down} is the down-quark mass matrix. Hence, $V_{\text{down}} = V$. Consequently, the up-quark mass matrix m_{up} is real and diagonal;
- in some $SO(10)$ models it holds that $m_{\text{up}} = m_D$. It follows that the bimaximal structure of m_ν originates from M_R , which is diagonalized by $M_R = V_R^* M_R^{\text{diag}} V_R^\dagger$.

This scenario has been outlined already in [5, 6]. With the indicated set of properties, we can express Eq. (5) as

$$U = V^\dagger U_{\text{bimax}} , \quad (19)$$

with U_{bimax} corresponding to bimaximal mixing, which will be precisely defined in Eq. (21). Moreover, Eq. (14) changes to

$$\tilde{m}_D = V_R^T m_D V \Rightarrow \begin{cases} \tilde{m}_D^\dagger \tilde{m}_D = V^\dagger \text{diag}(m_u^2, m_c^2, m_t^2) V & \text{for LFV} , \\ \tilde{m}_D \tilde{m}_D^\dagger = V_R^T \text{diag}(m_u^2, m_c^2, m_t^2) V_R^* & \text{for } \eta_B . \end{cases} \quad (20)$$

In the above equation we have given the two important matrices $\tilde{m}_D \tilde{m}_D^\dagger$ and $\tilde{m}_D^\dagger \tilde{m}_D$ describing leptogenesis and the branching ratios of the lepton flavor violating processes. Note however, that for the latter we have for now neglected the logarithmic dependence on the heavy neutrino masses.

3.1 Low Energy Neutrino Phenomenology

The matrix diagonalizing m_ν is called U_ν and corresponds to a bimaximal mixing matrix:

$$U_\nu = U_{\text{bimax}} = P_\nu \tilde{U}_{\text{bimax}} Q_\nu = \text{diag}(1, e^{i\phi}, e^{i\omega}) \begin{pmatrix} \frac{1}{\sqrt{2}} & \frac{1}{\sqrt{2}} & 0 \\ -\frac{1}{2} & \frac{1}{2} & \frac{1}{\sqrt{2}} \\ \frac{1}{2} & -\frac{1}{2} & \frac{1}{\sqrt{2}} \end{pmatrix} \text{diag}(1, e^{i\sigma}, e^{i\tau}) . \quad (21)$$

We have included two diagonal phase matrices P_ν and Q_ν . It has been shown in Ref. [11] that this is the most general form if all "unphysical" phases are rotated away. We have in total five phases, one phase in $U_\ell = V$ and four phases in U_ν . Note that Q_ν is "Majorana-like" [11], i.e., the phases σ and τ do not appear in neutrino oscillations, but contribute to the low energy Majorana phases. Multiplying the matrices of Eq. (8) and Eq. (21) yields for the oscillation parameters:

$$U = U_\ell^\dagger U_\nu = V^\dagger U_{\text{bimax}} \Rightarrow \begin{cases} \sin^2 \theta_{12} = \frac{1}{2} - \frac{\lambda}{\sqrt{2}} \cos \phi + \mathcal{O}(\lambda^3) , \\ |U_{e3}| = \frac{\lambda}{\sqrt{2}} + \mathcal{O}(\lambda^3) , \\ \sin^2 \theta_{23} = \frac{1}{2} - (A \cos(\omega - \phi) + \frac{1}{4}) \lambda^2 + \mathcal{O}(\lambda^4) , \\ J_{CP}^{\text{lep}} = \frac{\lambda}{4\sqrt{2}} \sin \phi + \mathcal{O}(\lambda^3) . \end{cases} \quad (22)$$

Apparently, Eq. (22) generates correlations between the observables. The solar neutrino mixing parameter depends on the CP phase ϕ , which originates from the neutrino sector and is to a very good approximation the phase governing leptonic CP violation in oscillation experiments. Note that in order to have solar neutrino mixing of the observed magnitude, the phase has to be close to zero or 2π . Approximately, at 3σ it should be below $\pi/4$ or above $7\pi/4$. The smallest solar neutrino mixing angle is obtained for $\phi = 0$ and the prediction for $\sin^2 \theta_{12}$ is

$$\sin^2 \theta_{12} \gtrsim 0.334 \quad (0.333, 0.332, 0.331) . \quad (23)$$

This value of $\sin^2 \theta_{12} \gtrsim 0.33$ has to be compared with the experimental 1σ (2σ) limit of $\sin^2 \theta_{12} \leq 0.33$ (0.37), showing a small conflict. Note that for the numerical values, as well as for the generation of the plots, which will be presented and discussed in the following, we did not use the approximate expressions in Eq. (22), but the exact formulae¹. Besides the phases, we also vary the parameters of the CKM matrix in their 1 , 2 and 3σ ranges (though in particular the error in λ is negligible), and also fix these parameters to their best-fit values. Even for the best-fit values of the CKM parameters, there results a range of values, which is caused by the presence of the unknown phases ϕ and ω . To a good approximation, $|U_{e3}|$ is the sine of the Cabibbo angle divided by $\sqrt{2}$, leading to a sharp prediction of $|U_{e3}|^2 = 0.0258$. Varying the phases and the CKM parameters, we find a range of

$$|U_{e3}| = 0.1607_{-0.0059, 0.0068, 0.0080, 0.0091}^{+0.0058, 0.0069, 0.0083, 0.0096}, \quad (24)$$

where we took the central value $\lambda/\sqrt{2} = 0.1607$. Recall that the 1σ (2σ) bound on $|U_{e3}|$ is 0.11 (0.17). Therefore, the prediction for $|U_{e3}|$ is incompatible with the current 1σ bound of $|U_{e3}|$ and even quite close to the 2σ limit. The experiments taking data in the next 5 to 10 years [31] will have to find a signal corresponding to non-vanishing $|U_{e3}|$ in order for this particular framework to survive. Leptonic CP violation is in leading order proportional to $\lambda \sin \phi$, which is five orders in units of λ larger than the J_{CP} of the quark sector. If the neutrino sector conserved CP , one would obtain $J_{CP}^{\text{lep}} = \frac{1}{8} A \eta \lambda^4$, which is still two orders of λ larger than the J_{CP} of the quark sector. If V was equal to the unit matrix, which corresponds to bimaximal mixing in the PMNS matrix, J_{CP}^{lep} would be zero. There is an interesting “sum-rule” between leptonic CP violation, solar neutrino mixing and $|U_{e3}|$:

$$\sin^2 \theta_{12} \simeq \frac{1}{2} - |U_{e3}| \cos \phi \simeq \frac{1}{2} \pm \sqrt{|U_{e3}|^2 - 16 (J_{CP}^{\text{lep}})^2}. \quad (25)$$

Overall, the experimental result of $\sin^2 \theta_{12} \simeq 0.31$ implies large $\cos \phi$, and therefore small $\sin \phi$, leading to small CP violating effects even though $|U_{e3}|$ is sizable. Atmospheric neutrino mixing stays very close to maximal and due to cancellations $\sin^2 \theta_{23} = \frac{1}{2}$ can always occur. If $\cos(\omega - \phi) = 1$, then $\sin^2 \theta_{23}$ takes its minimal value. We have seen above that the observed low value of the solar neutrino mixing angle requires $\phi \simeq 0$, so that $\omega \simeq 0$ is implied when θ_{23} is very close to maximal. The minimal and maximal values of $\sin^2 \theta_{23}$ are given by

$$\sin^2 \theta_{23} \geq 0.445 \text{ (0.444, 0.443, 0.442)} \text{ and } \sin^2 \theta_{23} \leq 0.531 \text{ (0.532, 0.533, 0.534)}. \quad (26)$$

Probing deviations from maximal mixing of order 10% could be possible in future experiments [31]. In Fig. 1 we show the correlations between the oscillation parameters which result from the relation $U = V^\dagger U_{\text{bimax}}$ in Eq. (22). We plot J_{CP}^{lep} , ϕ and $\sin^2 \theta_{23}$ against $\sin^2 \theta_{12}$, as well as $\sin^2 \theta_{23}$ against $|U_{e3}|$. We also indicate the current 1 , 2 and 3σ ranges of the oscillation parameters. This shows again that solar neutrino mixing is predicted to be

¹Note for instance that the next term in the expansion of $|U_{e3}|$ is of order $\lambda^3 \simeq 0.01$ and can contribute sizably.

close to its 1σ bound and $|U_{e3}|$ even close to its 2σ bound.

Now we turn to the neutrino observables outside the oscillation framework and comment on the consequences for neutrinoless double beta decay. The two invariants related to the Majorana phases are

$$\begin{aligned} S_1 &= \frac{\lambda}{2} \sin(\phi + \tau) + \frac{\lambda^2}{2\sqrt{2}} \sin \tau + \mathcal{O}(\lambda^3) , \\ S_2 &= \frac{\lambda}{2} \sin(\phi - \sigma + \tau) + \frac{\lambda^2}{2\sqrt{2}} \sin(\sigma - \tau) + \mathcal{O}(\lambda^3) . \end{aligned} \quad (27)$$

As expected, the two phases σ and τ in Q_ν only appear in these quantities. According to the parameterization of Eq. (6), we have $S_1 = -c_{12} c_{13} s_{13} s_\beta$ and $S_2 = s_{12} c_{13} s_{13} s_{\alpha-\beta}$. We can insert in Eq. (27) the expressions for the mixing angles from Eq. (22) to obtain in leading order $\sin \beta \simeq -\sin(\phi + \tau)$ and $\sin(\alpha - \beta) \simeq \sin(\phi - \sigma + \tau)$. Hence, the Majorana phase σ is related to the phase α in the parametrization of Eq. (6). It is interesting to study the form of the neutrino mass matrix, which is responsible for bimaximal mixing. It reads

$$\begin{aligned} m_\nu^{\text{bimax}} &= \begin{pmatrix} A & B e^{-i\phi} & -B e^{-i\omega} \\ \cdot & (D + \frac{A}{2}) e^{-2i\phi} & (D - \frac{A}{2}) e^{-i(\phi+\omega)} \\ \cdot & \cdot & (D + \frac{A}{2}) e^{-2i\omega} \end{pmatrix} \\ &= \begin{pmatrix} 1 & 0 & 0 \\ 0 & e^{-i\phi} & 0 \\ 0 & 0 & e^{-i\omega} \end{pmatrix} \begin{pmatrix} A & B & -B \\ \cdot & D + \frac{A}{2} & D - \frac{A}{2} \\ \cdot & \cdot & D + \frac{A}{2} \end{pmatrix} \begin{pmatrix} 1 & 0 & 0 \\ 0 & e^{-i\phi} & 0 \\ 0 & 0 & e^{-i\omega} \end{pmatrix} , \end{aligned} \quad (28)$$

where

$$A = \frac{1}{2} (m_1 + m_2 e^{-2i\sigma}) , \quad B = \frac{1}{2\sqrt{2}} (m_2 e^{-2i\sigma} - m_1) , \quad D = \frac{m_3 e^{-2i\tau}}{2} . \quad (29)$$

The inner matrix in Eq. (28) is diagonalized by a real and bimaximal rotation and the masses are obtained as

$$m_1 = A - \sqrt{2} B , \quad e^{-2i\sigma} m_2 = A + \sqrt{2} B , \quad e^{-2i\tau} m_3 = 2 D . \quad (30)$$

Up to now there has been no need to specify the neutrino mass ordering. This is however necessary in order to discuss neutrinoless double beta decay ($0\nu\beta\beta$) [32]. There are three extreme hierarchies often discussed; the normal hierarchy ($m_3 \simeq \sqrt{\Delta m_A^2} \gg m_2 \simeq \sqrt{\Delta m_\odot^2} \gg m_1$), the inverted hierarchy ($m_2 \simeq m_1 \simeq \sqrt{\Delta m_A^2} \gg m_3$) and the quasi-degenerate case ($m_1 \simeq m_2 \simeq m_3 \gg \sqrt{\Delta m_A^2}$). The effective mass which can be measured in $0\nu\beta\beta$ experiments is the ee element of m_ν in the charged lepton basis. To first order in λ one gets for a normal hierarchy that $\langle m \rangle \simeq \frac{1}{2} \sqrt{\Delta m_\odot^2} \lambda$. In case of an inverted hierarchy we have

$$\langle m \rangle \simeq \sqrt{\Delta m_A^2} \left| c_\sigma + \sqrt{2} s_\sigma s_\phi \lambda \right| . \quad (31)$$

The maximal (minimal) effective mass is obtained for $\sigma = 0$ ($\sigma = \pi/2$). On the other hand, we have $\langle m \rangle \simeq \sqrt{\Delta m_A^2} \sqrt{1 - \sin^2 2\theta_{12} \sin^2 \alpha}$ in terms of the usual parametrization [32]. Therefore, as is also obvious from the discussion following Eq. (27), σ will be closely related to the Majorana phase α . Similar considerations apply to the quasi-degenerate case.

3.2 Lepton Flavor Violation

Now we study the branching ratios of the LFV decays like $\mu \rightarrow e\gamma$ for this scenario. With our present assumptions we have that $m_D = m_{\text{up}} = \text{diag}(m_u, m_c, m_t)$. With this input and with Eq. (20) one easily obtains

$$\left| (\tilde{m}_D^\dagger \tilde{m}_D)_{21} \right|^2 \simeq A^4 m_t^4 (\eta^2 - (1 - \rho)^2) \lambda^{10} + \mathcal{O}(\lambda^{14}) . \quad (32)$$

Note that we have neglected the logarithmic dependence on M_i . The double ratios are²

$$R(21/31) \simeq A^2 \lambda^4 + \mathcal{O}(\lambda^8) \quad , \quad R(21/32) \simeq A^2 (\eta^2 - (1 - \rho)^2) \lambda^6 + \mathcal{O}(\lambda^{10}) . \quad (33)$$

The branching ratios behave according to

$$\text{BR}(\mu \rightarrow e\gamma) : \text{BR}(\tau \rightarrow e\gamma) : \text{BR}(\tau \rightarrow \mu\gamma) \simeq \lambda^6 : \lambda^2 : 1 \quad , \quad (34)$$

which is in agreement with Ref. [33].

In order to conduct a more precise study of the rates of the LFV processes, we recall that there is some dependence on the heavy neutrino masses, as encoded in the matrix $L = \delta_{ij} \ln M_X/M_i$ in Eq. (13). Hence, we need to evaluate the values of the heavy Majorana neutrino masses, i.e., we need to invert the see-saw formula $m_\nu = -m_D^T M_R^{-1} m_D$ and diagonalize M_R [34, 35, 36]. The light neutrino mass matrix is displayed in Eq. (28). With $m_D = m_{\text{up}} = \text{diag}(m_u, m_c, m_t)$ the heavy neutrino mass matrix reads:

$$-M_R = m_{\text{up}} m_\nu^{-1} m_{\text{up}} = P_\nu \begin{pmatrix} \tilde{A} m_u^2 & \tilde{B} m_u m_c & -\tilde{B} m_u m_t \\ \cdot & \left(\tilde{D} + \frac{\tilde{A}}{2} \right) m_c^2 & \left(\tilde{D} - \frac{\tilde{A}}{2} \right) m_c m_t \\ \cdot & \cdot & \left(\tilde{D} + \frac{\tilde{A}}{2} \right) m_t^2 \end{pmatrix} P_\nu \quad , \quad (35)$$

where

$$\tilde{A} = \frac{1}{2m_1} + \frac{e^{2i\sigma}}{2m_2} = \frac{A}{A^2 - 2B^2} \quad , \quad \tilde{B} = \frac{e^{2i\sigma}}{2\sqrt{2}m_2} - \frac{1}{2\sqrt{2}m_1} = \frac{-B}{A^2 - 2B^2} \quad , \quad \tilde{D} = \frac{e^{2i\tau}}{2m_3} = \frac{1}{4D} .$$

A , B and D are given in Eq. (29). The heavy Majorana mass matrix is related to the inverse of the light neutrino mass matrix and has for bimaximal mixing a very similar

²The relative magnitude of the branching ratios has in this scenario been estimated in Ref. [33]. Here we take the dependence on M_i and m_i carefully into account and study in addition their absolute magnitude.

form. Due to the very hierarchical structure of M_R , and if none of the elements vanish, the eigenvalues are quite easy to obtain (see also [36]):

$$\begin{aligned}
M_1 e^{i\phi_1} &\simeq \frac{m_u^2 (\tilde{A}^2 - 2\tilde{B}^2)}{\tilde{A}} = \frac{2m_u^2}{m_1 + m_2 e^{-2i\sigma}} \quad , \\
M_2 e^{i\phi_2} &\simeq 2m_c^2 \frac{\tilde{A}\tilde{D}}{\tilde{D} + \tilde{A}/2} = 2e^{2i(\sigma+\tau)} m_c^2 \frac{m_1 + m_2 e^{-2i\sigma}}{m_2 m_3 + m_1 m_3 e^{2i\sigma} + 2m_1 m_2 e^{2i\tau}} \quad , \\
M_3 e^{i\phi_3} &\simeq m_t^2 (\tilde{D} + \tilde{A}/2) = \frac{m_t^2}{4m_1 m_2 m_3} (2e^{2i\tau} m_1 m_2 + e^{2i\sigma} m_1 m_3 + m_2 m_3) \quad .
\end{aligned} \tag{36}$$

Here $M_{1,2,3}$ are real and positive, and $\phi_{1,2,3}$ denote the phases of the complex eigenvalues of the inner matrix in Eq. (35). We see that the values of the heavy Majorana masses depend on the phases σ and τ , which in turn are related to the low energy Majorana phases. The matrix V_R is defined via $M_R = V_R^* M_R^{\text{diag}} V_R^\dagger$, where $M_R^{\text{diag}} = \text{diag}(M_1, M_2, M_3)$ contains real and positive entries. We find

$$\begin{aligned}
V_R &= i P_\nu^* \tilde{V}_R R_\nu \quad , \quad \text{where} \\
\tilde{V}_R &\simeq \begin{pmatrix} 1 & \frac{m_u}{m_c} \frac{\tilde{B}}{\tilde{A}} & -\frac{m_u}{m_t} \frac{2\tilde{B}(\tilde{A}^2 - 2\tilde{B}^2)}{\tilde{A}(\tilde{A}^2 - 2\tilde{B}^2 + 2\tilde{A}\tilde{D}) - 4\tilde{B}^2\tilde{D}} \\ -\frac{m_u}{m_c} \frac{\tilde{B}}{\tilde{A}} & 1 & -\frac{m_c}{m_t} \frac{\tilde{A}(\tilde{A}^2 - 2\tilde{B}^2 - 2\tilde{A}\tilde{D}) + 4\tilde{B}^2\tilde{D}}{\tilde{A}(\tilde{A}^2 - 2\tilde{B}^2 + 2\tilde{A}\tilde{D}) - 4\tilde{B}^2\tilde{D}} \\ \frac{m_u}{m_t} \frac{\tilde{B}}{\tilde{A}} & \frac{m_c}{m_t} \frac{\tilde{A}(\tilde{A}^2 - 2\tilde{B}^2 - 2\tilde{A}\tilde{D}) + 4\tilde{B}^2\tilde{D}}{\tilde{A}(\tilde{A}^2 - 2\tilde{B}^2 + 2\tilde{A}\tilde{D}) - 4\tilde{B}^2\tilde{D}} & 1 \end{pmatrix} .
\end{aligned} \tag{37}$$

$R_\nu = \text{diag}(e^{-i\phi_1/2}, e^{-i\phi_2/2}, e^{-i\phi_3/2})$ contains the phases of the eigenvalues in Eq. (36). The above matrix is unitary to order m_u/m_c or m_c/m_t , which phenomenologically corresponds to an order of λ^4 . The heavy neutrino masses are plotted in Fig. 2 as a function of the lightest neutrino mass in case of normal ordering. Figure 3 shows the same for inversely ordered light neutrinos. We have chosen four different pairs of values for σ and τ . For the plots we have fixed Δm_\odot^2 and Δm_\oplus^2 to their best-fit values and have taken the quark masses as³ $m_u = 0.45$ MeV, $m_c = 1.2$ GeV and $m_t = 175$ GeV. The matrix M_R was diagonalized numerically. Eq. (36) is nevertheless an excellent approximation if σ and τ are far away from $\pi/2$. Moreover, it holds that $V_R \simeq \mathbb{1}$ in this case. On the other hand, if $\sigma \simeq \pi/2$ it can occur that M_1 and M_2 are almost degenerate if m_1 takes a value around 0.5 eV. This happens if $\tilde{A} = 0$ or, strictly speaking, $\tilde{A} m_u^2 \ll \tilde{B} m_u m_c$ in which case Eqs. (36, 37) are no longer valid [35, 36], but M_1 and M_2 build a pseudo-Dirac pair with mass

$$M_1 \simeq M_2 \simeq \tilde{B} m_u m_c \simeq \frac{m_u m_c}{2\sqrt{2} m_1} \sim 10^6 \text{ GeV} . \tag{38}$$

Note that the indicated value of m_1 is in conflict with tight cosmological constraints [37]. There are similar situations for M_2 and M_3 , which occur when $\tau \simeq \pi/2$. Neglecting these tuned cases, we plot the branching ratios in case of $\tau = \sigma = 0$ for the normal ordering in

³The values for the heavy neutrino masses are not much different when we take the quark masses at larger scale.

Fig. 4 as a function of the smallest neutrino mass⁴, choosing the SPS points 1a, 2 and 4. We do not use points 1b and 3, because the corresponding plots will be indistinguishable from the plots for points 1a and 2, respectively. The results are typical if both τ and σ are not close to $\pi/2$. Due to the presence of the diagonal matrix $L = \delta_{ij} \ln M_X/M_i$ in the equation for the branching ratios the possibility of cancellations arises, leading to a very small branching ratio. From Eq. (32), such a cancellation is impossible. We have also indicated current and future sensitivities on the decays in Fig. 4. Typically, $\mu \rightarrow e\gamma$ can be observable for neutrino masses above 10^{-3} eV, unless the SUSY masses approach the TeV scale. The decay $\tau \rightarrow e\gamma$ is predicted to be very small, and $\tau \rightarrow \mu\gamma$ requires rather large neutrino masses and small SUSY masses. This is illustrated in Fig. 5, where we have plotted the branching ratios as a function of the SUSY parameter $m_{1/2}$ for the SPS slopes 1a and 2 from Table 1. We have chosen two values for the neutrino masses (normal ordering), namely 0.002 eV and 0.2 eV. The relative magnitude of the branching ratios, as estimated in Eq. (34), holds true for most of the parameter space.

3.3 Comments on Leptogenesis

It is worth to discuss leptogenesis in the scenario under study. As indicated in Sec. 2.3, the value of the baryon asymmetry crucially depends on the spectrum of the heavy Majorana neutrinos, which we have displayed in Figs. 2 and 3 for normally and inversely ordered light neutrino masses. It also depends on the matrix V_R , which in case of σ far away from $\pi/2$ is given in Eq. (37). We note here that P_ν does not play a role for leptogenesis, since $\tilde{m}_D \tilde{m}_D^\dagger = R \tilde{V}_R^T \text{diag}(m_u^2, m_c^2, m_t^2) \tilde{V}_R^* R^*$. As the neutrino oscillation Dirac phase which was identified with ϕ appears in P_ν , we have the interesting result that the low energy Majorana phases can be relevant for leptogenesis, which indeed turns out to be the case. If σ is far away from $\pi/2$, the eigenvalues are strongly hierarchical. In general M_1 does not exceed 10^6 GeV, as obvious from Eq. (36) and Figs. 2, 3. According to Eq. (18) this is too small a value for successful thermal leptogenesis. We mentioned in Sec. 2.3 two solutions to this problem, namely resonant and non-thermal leptogenesis. The first possibility occurs for $\sigma \simeq \pi/2$, where two heavy neutrinos have quasi-degenerate masses, see Eq. (38). In Ref. [36] a similar framework was considered, and the mass splitting required to generate an η_B of the observed size has been estimated. The result corresponds to $|1 - M_2/M_1| \simeq 10^{-5} \dots 10^{-6}$, which is a rather fine-tuned situation. However, there are two rather interesting aspects to this case: as discussed in Section 3.1 the phase σ is related to the low energy Majorana phase α . If $\alpha = \pi/2$ it is known that for quasi-degenerate neutrinos the stability with respect to radiative corrections is significantly improved [24]. Moreover, the resonant condition occurs if the smallest neutrino mass is approximately 0.5 eV, i.e., the light neutrinos are quasi-degenerate. In this case the effective mass for

⁴Note that for inverse mass ordering the masses m_1 and m_2 are always rather close. As obvious from Eq. (36), this leads to slightly larger masses for the heavy neutrinos. This translates into branching ratios which for small m_3 are larger by a factor of roughly 3.

neutrinoless double beta decay reads

$$\langle m \rangle \simeq m_1 \left(\sqrt{2} \lambda + \frac{1}{2} c_{\phi+2\tau} \lambda^2 \right). \quad (39)$$

The maximum value of the effective mass for quasi-degenerate neutrinos is roughly m_1 [32]. Therefore there are sizable cancellations in the effective mass [38] when the resonance condition for the heavy neutrino masses is fulfilled. With $m_1 \simeq 0.5$ eV we can predict that $\langle m \rangle \simeq 0.16$ eV, a value which can be easily tested in running and up-coming experiments [39]. If $\tau \simeq \pi/2$, it is apparent from Figs. 2 and 3 that situations can occur in which M_2 and M_3 are quasi-degenerate. Hence, their decay could create a resonantly enhanced decay asymmetry, but the lighter neutrino with mass M_1 should not wash out this asymmetry. Determining if this is indeed possible would require a dedicated study and solution of the Boltzmann equations, but successful leptogenesis would undoubtedly correspond to a very unusual situation.

Leaving the fine-tuned possibility of resonant leptogenesis aside, we can consider non-thermal leptogenesis. However, as also discussed in Ref. [36], the decay asymmetry ε_1 turns out to be too tiny: if we insert the phenomenological values $m_u/m_c \sim m_c/m_t \simeq \lambda^4$ in the exact equations and if we refrain from considering the possibility of resonant enhancements, ε_1 is of order $\lambda^{16} \simeq 10^{-11}$. In principle, the baryon asymmetry could be generated by the decays of the heavier neutrinos, i.e., by ε_2 and/or ε_3 , which are indeed larger than ε_1 . This possibility would indicate that the inflaton has a sizable branching ratio in the heavier neutrinos. However, this would also require that the lightest Majorana neutrino N_1 does not wash out the asymmetry generated by N_2 and N_3 , which in turn would require rather special conditions (see the comments about resonant leptogenesis from above). We conclude that leptogenesis in this realization of QLC is only possible in case of highly fine-tuned conditions.

4 Second Realization of QLC

In this section we discuss another possible realization of QLC, which has also been outlined already in [5, 6]:

- the conventional see-saw mechanism generates the neutrino mass matrix. Diagonalization of m_ν is achieved via $m_\nu = U_\nu^* m_\nu^{\text{diag}} U_\nu^\dagger$ and U_ν is related to V (in the sense that $U_\nu^\dagger = P_\nu V Q_\nu$);
- the matrix diagonalizing the charged leptons corresponds to bimaximal mixing: $U_\ell = U_{\text{bimax}}^T$. This can be achieved when $V_{\text{up}} = V^\dagger$, therefore $V_{\text{down}} = \mathbb{1}$;
- if indeed $V_{\text{up}} = V^\dagger$, then $m_\nu = -m_D^T M_R^{-1} m_D$ is diagonalized by the CKM matrix. If M_R does not introduce additional rotations we can have the $SO(10)$ -like relation

$m_{\text{up}} = m_D = V'_{\text{up}} m_{\text{up}}^{\text{diag}} P_\nu V Q_\nu$. Here V'_{up} denotes in our convention the in principle unknown right-handed rotation of m_D . The condition of M_R not introducing additional rotations means that $V_R = (V'_{\text{up}})^*$, where $M_R = V_R^* M_R^{\text{diag}} V_R^\dagger$.

In the following we will redo the calculations of the previous sections for all the observables with this second set of assumptions. First of all we note that in the important basis in which the charged leptons and heavy neutrinos are real and diagonal the Dirac mass matrix reads

$$\begin{aligned} m_D &\rightarrow \tilde{m}_D = V_R^T m_D U_\ell = m_{\text{up}}^{\text{diag}} P_\nu V Q_\nu U_{\text{bimax}}^T \\ \Rightarrow \begin{cases} \tilde{m}_D^\dagger \tilde{m}_D = U_{\text{bimax}} Q_\nu^\dagger V^\dagger \text{diag}(m_u^2, m_c^2, m_t^2) V Q_\nu U_{\text{bimax}}^T & \text{for LFV} , \\ \tilde{m}_D \tilde{m}_D^\dagger = \text{diag}(m_u^2, m_c^2, m_t^2) & \text{for } \eta_B . \end{cases} \end{aligned} \quad (40)$$

We note here that the diagonal form of $\tilde{m}_D \tilde{m}_D^\dagger$ means that there is no leptogenesis in this realization of QLC. The correspondence between the light and heavy Majorana neutrino masses is rather trivial:

$$M_1 = \frac{m_u^2}{m_1} , \quad M_2 = \frac{m_c^2}{m_2} , \quad M_3 = \frac{m_t^2}{m_3} . \quad (41)$$

In Fig. 6 we show the neutrino masses as a function of the smallest neutrino mass m_1 and m_3 for the normal and inverted ordering, respectively. Again, we have taken the best-fit points for Δm_{\odot}^2 and Δm_{A}^2 and the quark masses are $m_u = 0.45$ MeV, $m_c = 1.2$ GeV and $m_t = 175$ GeV.

4.1 Low Energy Neutrino Phenomenology

In our second case the PMNS matrix can be written as

$$U = U_\ell^\dagger U_\nu = R_{23} R_{12} (P_\nu V Q_\nu)^\dagger , \quad (42)$$

where R_{ij} is a rotation with $\pi/4$ around the (ij) -axis and P_ν and Q_ν are defined in Eq. (21). We remark that an analysis of this framework including all possible phases has not been performed before (see Refs. [5, 6, 9]). With our parametrization of the PMNS matrix the two phases in P_ν are ‘‘Majorana-like’’ and do not show up in oscillations. All phases originate from the neutrino sector. The neutrino oscillation observables are

$$\begin{aligned} \sin^2 \theta_{12} &= \frac{1}{2} - \lambda \cos \sigma + \mathcal{O}(\lambda^3) , \\ |U_{e3}| &= \frac{A}{\sqrt{2}} \lambda^2 + \mathcal{O}(\lambda^3) , \\ \sin^2 \theta_{23} &= \frac{1}{2} - \sqrt{\frac{1}{2}} A \lambda^2 \cos(\tau - \sigma) + \mathcal{O}(\lambda^3) , \\ J_{CP}^{\text{lep}} &= \frac{\lambda^2}{4\sqrt{2}} \sin(\tau - \sigma) + \mathcal{O}(\lambda^3) . \end{aligned} \quad (43)$$

The solar neutrino mixing parameter depends on the CP phase σ . Note that in order to have solar neutrino mixing of the observed magnitude, the phase has to be close to zero or 2π , at 3σ typically below $\pi/4$ (or above $7\pi/4$). The prediction for $\sin^2 \theta_{12}$ is⁵

$$\sin^2 \theta_{12} \gtrsim 0.279 \text{ (0.278, 0.277, 0.276)} . \quad (44)$$

These are lower values than in our first scenario. The numbers have to be compared to the 1σ (2σ) limit of $\sin^2 \theta_{12} \leq 0.33$ (0.37). The parameter $|U_{e3}|$ has a ‘‘central value’’ of $A\lambda^2/\sqrt{2} \simeq 0.0295$. In the first scenario the prediction was $|U_{e3}|^2 = 0.0258$, which is by chance almost the same number. We find a range of

$$|U_{e3}| = 0.0295_{-0.0058, 0.0066, 0.0076, 0.0084}^{+0.0059, 0.0070, 0.0085, 0.0099} . \quad (45)$$

Recall that the 1σ (2σ) bound on $|U_{e3}|$ is 0.11 (0.17). Probing such small values of $|U_{e3}|$ is rather challenging and would require at least superbeams [31]. Due to cancellations $\sin^2 \theta_{23} = \frac{1}{2}$ can always occur. In this case, $\cos(\tau - \sigma) = 0$ and J_{CP}^{lep} takes its maximal possible value. The minimal and maximal values of $\sin^2 \theta_{23}$ are given by

$$\sin^2 \theta_{23} \geq 0.466 \text{ (0.465, 0.463, 0.462)} \text{ and } \sin^2 \theta_{23} \leq 0.536 \text{ (0.538, 0.539, 0.540)} , \quad (46)$$

which is only a slightly larger range compared to the first scenario, and thus hard to probe experimentally. Leptonic CP violation is in leading order proportional to $\lambda^2 \sin(\tau - \sigma)$, which is four powers of λ larger than the J_{CP} of the quark sector. If the neutrino sector conserved CP , then J_{CP}^{lep} vanishes. Note that the phase combination $(\tau - \sigma)$ governs the magnitude of the atmospheric neutrino mixing. In the first scenario, J_{CP}^{lep} and the solar neutrino mixing were correlated in this way. In analogy to Eq. (25) we can write the sum-rule

$$\sin^2 \theta_{23} \simeq \frac{1}{2} - |U_{e3}| \cos(\tau - \sigma) \simeq \frac{1}{2} \pm \sqrt{|U_{e3}| - 16 J_{CP}^2} . \quad (47)$$

In Fig. 7 we show the correlations between the oscillation parameters which result from the relation in Eq. (42). We plot J_{CP}^{lep} and $\sin^2 \theta_{12}$ against $\sin^2 \theta_{23}$, as well as σ and $|U_{e3}|$ against $\sin^2 \theta_{12}$. We also indicate the current 1, 2 and 3σ ranges of the oscillation parameters, showing that the predictions of this scenario are perfectly compatible with all current data.

Turning aside again from the oscillation observables, the invariants for the Majorana phases are

$$S_1 = -\frac{\lambda^2}{2} A \sin(\sigma + \omega) + \mathcal{O}(\lambda^3) \text{ and } S_2 = -\frac{\lambda^2}{2} A \sin(\omega - \phi) + \mathcal{O}(\lambda^3) . \quad (48)$$

In analogy to the discussion following Eq. (27), we can translate these formulae into expressions for the low energy Majorana phases α and β . This leads to $\sin \beta \simeq \sin(\sigma + \omega)$ and

⁵Again, we do not use the approximate expressions in Eq. (43), but the exact equations. Besides the phases, we also vary the parameters of the CKM matrix in their 1, 2 and 3σ ranges, and also fix these parameters to their best-fit values.

$\sin(\alpha - \beta) \simeq \sin(\omega - \phi)$ and indicates that α in the parametrization of Eq. (6) is related to $(\phi + \sigma)$. Indeed, a calculation of the effective mass in case of an inverted hierarchy, where the Majorana phase α plays a crucial role [32], results in

$$\langle m \rangle \simeq \sqrt{\Delta m_A^2} \left| c_{\phi+\sigma} + 2 \frac{s_\phi}{c_{\phi+\sigma}} \lambda^2 \right|. \quad (49)$$

Similar statements can be made for quasi-degenerate neutrinos.

4.2 Lepton Flavor Violation

With the help of Eqs. (13, 40) we can evaluate the branching ratios for LFV processes, ignoring for the moment the logarithmic dependence on the heavy neutrino masses. The decay $\mu \rightarrow e\gamma$ is found to be governed by

$$\left| (\tilde{m}_D^\dagger \tilde{m}_D)_{21} \right|^2 \simeq \frac{1}{4} A^2 m_t^4 \lambda^4 + \mathcal{O}(\lambda^5). \quad (50)$$

Comparing with Eq. (32) we see that in the second realization the branching ratio is larger than in the first realization by 6 inverse powers of λ , or $\lambda^{-6} \simeq 8820$, almost 4 orders of magnitude. For the double ratios of the branching ratios we obtain

$$R(21/31) \simeq 1 - 2\sqrt{2} A \cos(\sigma - \tau) \lambda^2 + \mathcal{O}(\lambda^3) \quad , \quad R(21/32) \simeq A^2 \lambda^4 + \mathcal{O}(\lambda^5). \quad (51)$$

There is a small dependence on the phase combination $(\sigma - \tau)$, which also governs leptonic CP violation in oscillation experiments and the magnitude of the atmospheric neutrino mixing angle. The branching ratios behave according to

$$\text{BR}(\mu \rightarrow e\gamma) : \text{BR}(\tau \rightarrow e\gamma) : \text{BR}(\tau \rightarrow \mu\gamma) \simeq A^2 \lambda^4 : A^2 \lambda^4 : 1. \quad (52)$$

In Fig. 8 we show the branching ratios for $\mu \rightarrow e\gamma$, $\tau \rightarrow e\gamma$ and $\tau \rightarrow \mu\gamma$ as a function of the smallest neutrino mass for a normal mass ordering, choosing the SPS points 1a, 2 and 4. The small dependence on the heavy neutrino masses is taken into account and plots for the inverted ordering look very similar. Note that from Fig. 8 it follows that the dependence on the neutrino masses is very small. The relative magnitude of the branching ratios, as estimated in Eq. (51), holds true to a very high accuracy. However, we immediately see that the prediction for $\mu \rightarrow e\gamma$ is at least one order of magnitude above the current limit. To obey the experimental limit on $\text{BR}(\mu \rightarrow e\gamma)$, the SUSY masses should be in the several TeV range. This is illustrated in Fig. 9, where we have plotted the branching ratios as a function of the SUSY parameter $m_{1/2}$ for the SPS slopes 1a and 2 from Table 1. We took the normal ordering of neutrino masses with a smallest mass $m_1 = 0.02$ eV. Once we have adjusted the SUSY parameters to have $\text{BR}(\mu \rightarrow e\gamma)$ below its current limit, the other decays $\tau \rightarrow e\gamma$ and $\tau \rightarrow \mu\gamma$ are too rare to be observed with presently planned experiments.

5 Conclusions and Summary

We have considered the phenomenology of two predictive see-saw scenarios leading approximately to Quark-Lepton Complementarity. Both have in common that bimaximal mixing is corrected by the CKM matrix. We have studied the complete low energy phenomenology, including the neutrino oscillation parameters, where we have taken into account all possible phases, and neutrinoless double beta decay. Moreover, lepton flavor violating charged lepton decays have been studied and all results have been compared to presently available and expected future data. Finally, we have commented on the possibility of leptogenesis.

In terms of the elements of the PMNS matrix U and the CKM matrix V , the QLC condition can be written as $|U_{e2}| + |V_{ud}| = 1/\sqrt{2}$. This defines the solar neutrino mixing parameter $\sin^2 \theta_{12}$ to be $\sin^2(\frac{\pi}{4} - \lambda)$. Taking the best-fit, as well as the 1, 2 and 3σ values of λ from Eq. (9) we obtain

$$\sin^2 \theta_{12} = 0.2805 \pm (0.0009, 0.0018, 0.0027) . \quad (53)$$

A second QLC relation has also been suggested, namely $\theta_{23} + A\lambda^2 = \pi/4$, which is the analogue of Eq. (2) for the (23)-sector. This can also be written as $|U_{\mu 3}| + |V_{cb}| = 1/\sqrt{2}$ and its precise prediction is

$$\sin^2 \theta_{23} = 0.4583_{-0.0011, 0.0022, 0.0034}^{+0.0011, 0.0022, 0.0032} . \quad (54)$$

We remark that in our scenario with all possible CP phases the above two relations correspond to at least one phase being zero.

The first scenario has bimaximal mixing from the neutrino sector and the matrix diagonalizing the charged leptons is the CKM matrix. The main results are:

- solar neutrino mixing is predicted close to its 1σ bound and $|U_{e3}|$ even close to its 2σ bound, see Fig. 1. The phase governing the magnitude of θ_{12} is the CP phase of neutrino oscillations and is implied to be small;
- $|U_{e3}|$ is roughly 0.16, i.e., it should be observed soon;
- the lowest value of $\sin^2 \theta_{12}$ (corresponding to CP conservation) is roughly 0.33, which differs by about 15% from Eq. (53). For $\sin^2 \theta_{23}$ the lowest value is 0.44, in moderate agreement with Eq. (54);
- the decay $\mu \rightarrow e\gamma$ can be observable for neutrino masses above 10^{-3} eV, unless the SUSY masses approach the TeV scale. The decay $\tau \rightarrow e\gamma$ is predicted to be very small, and $\tau \rightarrow \mu\gamma$ requires rather large neutrino masses. The relative magnitude of the branching ratios is $\text{BR}(\mu \rightarrow e\gamma) : \text{BR}(\tau \rightarrow e\gamma) : \text{BR}(\tau \rightarrow \mu\gamma) \simeq \lambda^6 : \lambda^2 : 1$;
- successful leptogenesis depends on the low energy Majorana phases but is fine-tuned. One possibility occurs if $\sigma \simeq \pi/2$, leading to two quasi-degenerate heavy neutrinos

masses. It also leads to quasi-degenerate light neutrinos with mass around 0.5 eV and to sizable cancellations in neutrinoless double beta decay, corresponding to $\langle m \rangle \simeq 0.16$ eV.

The second scenario has bimaximal mixing from the charged lepton sector and the matrix diagonalizing the neutrinos is the CKM matrix. The main results are:

- the neutrino oscillation parameters are perfectly compatible with all data, see Fig. 7. The phase governing the magnitude of θ_{23} is the CP phase of neutrino oscillations;
- $|U_{e3}|$ is roughly 0.03, which is a rather small value setting a challenge for future experiments;
- the lowest value of $\sin^2 \theta_{12}$ (corresponding to CP conservation) is roughly 0.28, in perfect agreement with Eq. (53). For $\sin^2 \theta_{23}$ the lowest value is 0.46 (but θ_{23} can be maximal), in perfect agreement with Eq. (54). If $\sin^2 \theta_{23} = \frac{1}{2}$ then maximal CP violation is implied;
- The branching ratio of $\mu \rightarrow e\gamma$ is larger than in the first scenario by six inverse powers of λ and therefore typically too large unless the SUSY masses are of several TeV scale. If they are so heavy that $\mu \rightarrow e\gamma$ is below its current limit, $\tau \rightarrow e\gamma$ and $\tau \rightarrow \mu\gamma$ are too small to be observed. The relative magnitude of the branching ratios is $\text{BR}(\mu \rightarrow e\gamma) : \text{BR}(\tau \rightarrow e\gamma) : \text{BR}(\tau \rightarrow \mu\gamma) \simeq A^2 \lambda^4 : A^2 \lambda^4 : 1$;
- there can be no leptogenesis.

We conclude that both scenarios predict interesting and easily testable phenomenology. However, the first scenario is in slight disagreement with oscillation data and allows leptogenesis only for fine-tuned parameter values. In the second scenario the predictions for LFV decays are in contradiction to experimental results unless the SUSY parameters are very large. Moreover no leptogenesis is possible in this case.

Acknowledgments

We thank J. Klinsmann for invaluable encouragement. This work was supported by the “Deutsche Forschungsgemeinschaft” in the “Sonderforschungsbereich 375 für Astroteilchenphysik” and under project number RO-2516/3-1 (W.R.).

References

- [1] R. N. Mohapatra *et al.*, hep-ph/0510213; R. N. Mohapatra and A. Y. Smirnov, hep-ph/0603118; A. Strumia and F. Vissani, hep-ph/0606054.
- [2] W. Rodejohann, Phys. Rev. D **69**, 033005 (2004).

- [3] F. Vissani, hep-ph/9708483; V. D. Barger, S. Pakvasa, T. J. Weiler and K. Whisnant, Phys. Lett. B **437**, 107 (1998); A. J. Baltz, A. S. Goldhaber and M. Goldhaber, Phys. Rev. Lett. **81**, 5730 (1998); H. Georgi and S. L. Glashow, Phys. Rev. D **61**, 097301 (2000); R. N. Mohapatra and S. Nussinov, Phys. Rev. D **60**, 013002 (1999); I. Stancu and D. V. Ahluwalia, Phys. Lett. B **460**, 431 (1999).
- [4] T. Schwetz, Acta Phys. Polon. B **36**, 3203 (2005), hep-ph/0510331; M. Maltoni *et al.*, New J. Phys. **6**, 122 (2004), hep-ph/0405172v5.
- [5] M. Raidal, Phys. Rev. Lett. **93**, 161801 (2004).
- [6] H. Minakata and A. Y. Smirnov, Phys. Rev. D **70**, 073009 (2004).
- [7] P. H. Frampton and R. N. Mohapatra, JHEP **0501**, 025 (2005); S. K. Kang, C. S. Kim and J. Lee, Phys. Lett. B **619**, 129 (2005); N. Li and B. Q. Ma, Phys. Rev. D **71**, 097301 (2005); K. Cheung *et al.*, Phys. Rev. D **72**, 036003 (2005); Z. Z. Xing, Phys. Lett. B **618**, 141 (2005); A. Datta, L. Everett and P. Ramond, Phys. Lett. B **620**, 42 (2005); S. Antusch, S. F. King and R. N. Mohapatra, Phys. Lett. B **618**, 150 (2005); N. Li and B. Q. Ma, Eur. Phys. J. C **42**, 17 (2005); T. Ohlsson, Phys. Lett. B **622**, 159 (2005); D. Falcone, hep-ph/0509028. L. L. Everett, Phys. Rev. D **73**, 013011 (2006); A. Dighe, S. Goswami and P. Roy, Phys. Rev. D **73**, 071301 (2006); B. C. Chauhan *et al.*, hep-ph/0605032; F. Gonzalez-Canales and A. Mondragon, hep-ph/0606175.
- [8] J. Ferrandis and S. Pakvasa, Phys. Lett. B **603**, 184 (2004); Phys. Rev. D **71**, 033004 (2005).
- [9] C. A. de S. Pires, J. Phys. G **30**, B29 (2004); N. Li and B. Q. Ma, Eur. Phys. J. C **42**, 17 (2005).
- [10] M. Jezabek and Y. Sumino, Phys. Lett. B **457**, 139 (1999); Z. Z. Xing, Phys. Rev. D **64**, 093013 (2001); C. Giunti and M. Tanimoto, Phys. Rev. D **66**, 053013 (2002); Phys. Rev. D **66**, 113006 (2002); S. T. Petcov and W. Rodejohann, Phys. Rev. D **71**, 073002 (2005); J. Ferrandis and S. Pakvasa, Phys. Lett. B **603**, 184 (2004); S. Antusch and S. F. King, Phys. Lett. B **631**, 42 (2005).
- [11] P. H. Frampton, S. T. Petcov and W. Rodejohann, Nucl. Phys. B **687**, 31 (2004).
- [12] P. Minkowski, Phys. Lett. B **67**, 421 (1977); M. Gell-Mann, P. Ramond, and R. Slansky in *Supergravity*, p. 315, edited by F. Nieuwenhuizen and D. Friedman, North Holland, Amsterdam, 1979; T. Yanagida, Proc. of the *Workshop on Unified Theories and the Baryon Number of the Universe*, edited by O. Sawada and A. Sugamoto, KEK, Japan 1979; R. N. Mohapatra and G. Senjanovic, Phys. Rev. Lett. **44**, 912 (1980).
- [13] S. M. Bilenky, J. Hosek and S. T. Petcov, Phys. Lett. B **94**, 495 (1980); J. Schechter and J. W. F. Valle, Phys. Rev. D **22**, 2227 (1980); Phys. Rev. D **23**, 1666 (1981); M. Doi *et al.*, Phys. Lett. B **102**, 323 (1981).

- [14] L. Wolfenstein, Phys. Rev. Lett. **51**, 1945 (1983).
- [15] J. Charles *et al.* [CKMfitter Group], Eur. Phys. J. C **41**, 1 (2005); A. Hocker and Z. Ligeti, hep-ph/0605217.
- [16] C. Jarlskog, Phys. Rev. Lett. **55**, 1039 (1985).
- [17] J. F. Nieves and P. B. Pal, Phys. Rev. D **36**, 315 (1987); Phys. Rev. D **64**, 076005 (2001); J. A. Aguilar-Saavedra and G. C. Branco, Phys. Rev. D **62**, 096009 (2000).
- [18] S. T. Petcov, Sov. J. Nucl. Phys. **25**, 340 (1977) [Yad. Fiz. **25**, 641 (1977 ER-RAT,25,698.1977 ERRAT,25,1336.1977)]; S. M. Bilenky, S. T. Petcov and B. Pontecorvo, Phys. Lett. B **67**, 309 (1977); T. P. Cheng and L. F. Li, Phys. Rev. Lett. **45**, 1908 (1980).
- [19] F. Borzumati and A. Masiero, Phys. Rev. Lett. **57**, 961 (1986); J. Hisano, T. Moroi, K. Tobe and M. Yamaguchi, Phys. Rev. D **53**, 2442 (1996); J. A. Casas and A. Ibarra, Nucl. Phys. B **618**, 171 (2001).
- [20] M. L. Brooks *et al.* [MEGA Collaboration], Phys. Rev. Lett. **83**, 1521 (1999).
- [21] L. M. Barkov *et al.*, the MEG Proposal (1999), <http://meg.psi.ch>.
- [22] S. T. Petcov *et al.*, Nucl. Phys. B **676**, 453 (2004).
- [23] B. C. Allanach *et al.*, Eur. Phys. J. C **25**, 113 (2002) [eConf **C010630**, P125 (2001)].
- [24] See for instance S. Antusch *et al.*, JHEP **0503**, 024 (2005).
- [25] D. N. Spergel *et al.*, astro-ph/0603449.
- [26] M. Fukugita and T. Yanagida, Phys. Lett. B **174**, 45 (1986).
- [27] W. Buchmüller, P. Di Bari and M. Plümacher, New J. Phys. **6**, 105 (2004), hep-ph/0406014.
- [28] G. F. Giudice *et al.*, Nucl. Phys. B **685**, 89 (2004).
- [29] M. Flanz, E. A. Paschos and U. Sarkar, Phys. Lett. B **345**, 248 (1995) [Erratum-ibid. B **382**, 447 (1996)]; M. Flanz, E. A. Paschos, U. Sarkar and J. Weiss, Phys. Lett. B **389**, 693 (1996); A. Pilaftsis, Phys. Rev. D **56**, 5431 (1997); W. Buchmüller and M. Plümacher, Phys. Lett. B **431**, 354 (1998); E. Roulet, L. Covi and F. Vissani, Phys. Lett. B **424**, 101 (1998); A. Pilaftsis and T. E. J. Underwood, Nucl. Phys. B **692**, 303 (2004); A. Anisimov, A. Broncano and M. Plümacher, Nucl. Phys. B **737**, 176 (2006).

- [30] G. Lazarides and Q. Shafi, Phys. Lett. B **258**, 305 (1991); K. Kumekawa, T. Moroi and T. Yanagida, Prog. Theor. Phys. **92**, 437 (1994); G. F. Giudice, M. Peloso, A. Riotto and I. Tkachev, JHEP **9908**, 014 (1999); T. Asaka, K. Hamaguchi, M. Kawasaki and T. Yanagida, Phys. Lett. B **464**, 12 (1999); Phys. Rev. D **61**, 083512 (2000); T. Asaka, H. B. Nielsen and Y. Takanishi, Nucl. Phys. B **647**, 252 (2002).
- [31] For an overview on future experiments and their sensitivity, see e.g., A. Blondel, *et al.*, hep-ph/0606111; S. Choubey, hep-ph/0509217.
- [32] Recent analyzes of neutrinoless double beta decay are: S. Pascoli, S. T. Petcov and T. Schwetz, Nucl. Phys. B **734**, 24 (2006); S. Choubey and W. Rodejohann, Phys. Rev. D **72**, 033016 (2005); A. de Gouvea and J. Jenkins, hep-ph/0507021; M. Lindner, A. Merle and W. Rodejohann, Phys. Rev. D **73**, 053005 (2006).
- [33] K. Cheung *et al.*, in Ref. [7].
- [34] D. Falcone and F. Tramontano, Phys. Rev. D **63**, 073007 (2001); G. C. Branco, R. Gonzalez Felipe, F. R. Joaquim and M. N. Rebelo, Nucl. Phys. B **640**, 202 (2002); D. Falcone, Phys. Rev. D **68**, 033002 (2003).
- [35] E. Nezri and J. Orloff, JHEP **0304**, 020 (2003).
- [36] E. K. Akhmedov, M. Frigerio and A. Y. Smirnov, JHEP **0309**, 021 (2003).
- [37] For a recent review, see S. Hannestad, hep-ph/0602058.
- [38] W. Rodejohann, Nucl. Phys. B **597**, 110 (2001).
- [39] C. Aalseth *et al.*, hep-ph/0412300.

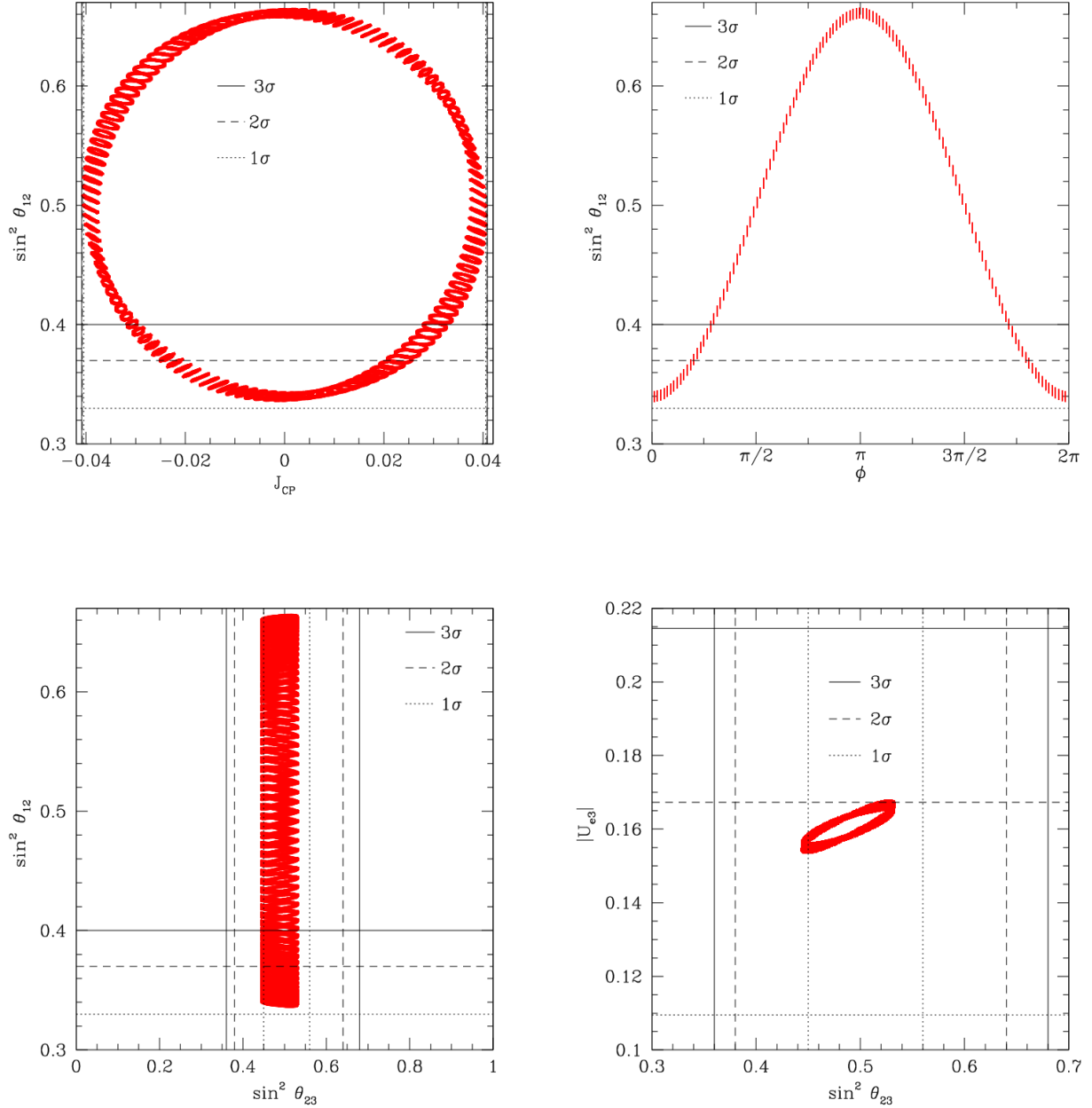


Figure 1: First realization of QLC: neutrino observables resulting from Eq. (22) for the 3σ ranges of the CKM parameters. We also indicated the present 1, 2 and 3σ ranges of the oscillation parameters.

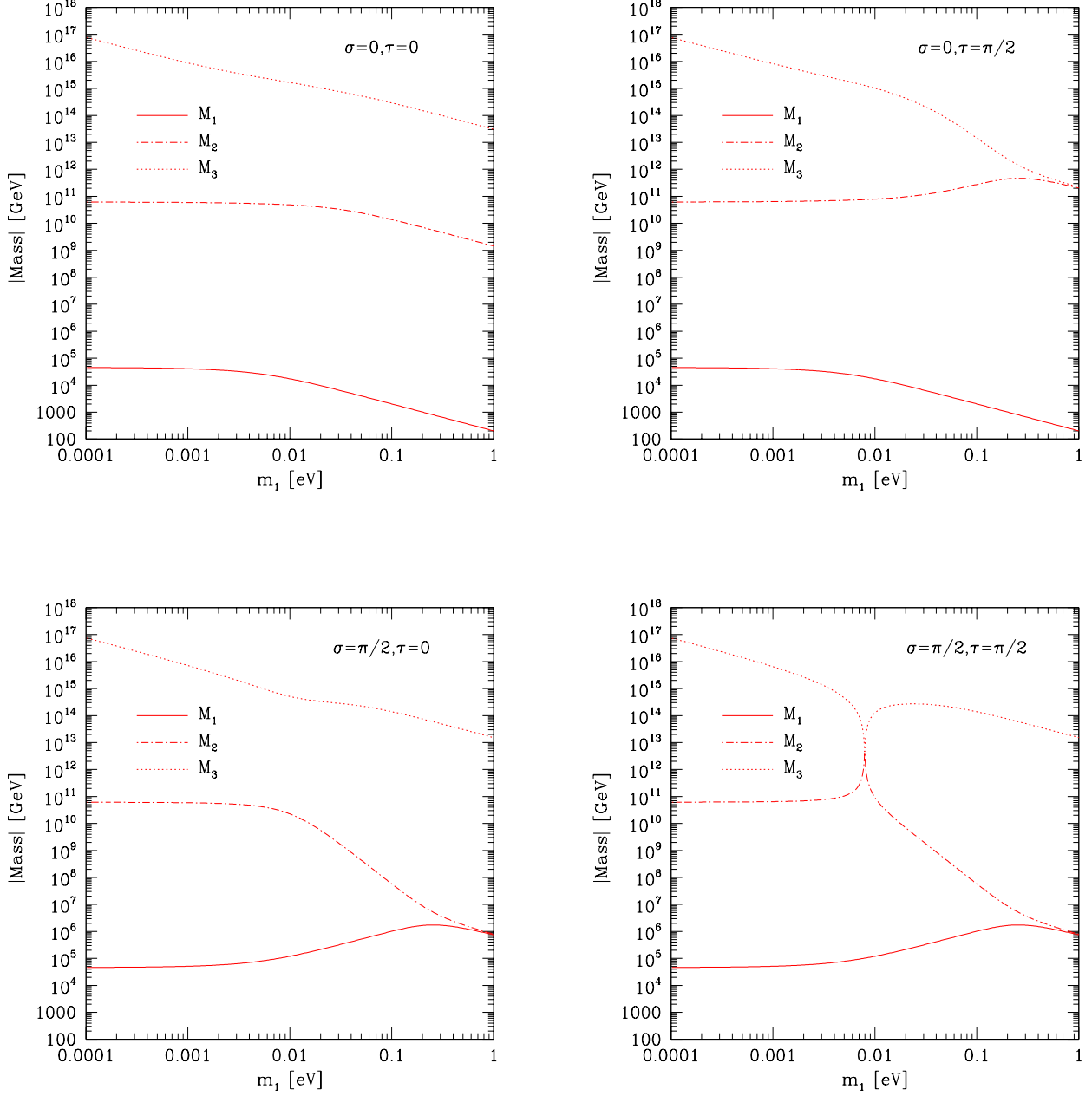


Figure 2: First realization of QLC: the heavy neutrino masses resulting from the diagonalization of Eq. (35) as a function of the smallest neutrino mass for the normal mass ordering. We have chosen four different pairs of values for σ and τ , showing the possible degeneracy of the masses. See text for further discussion.

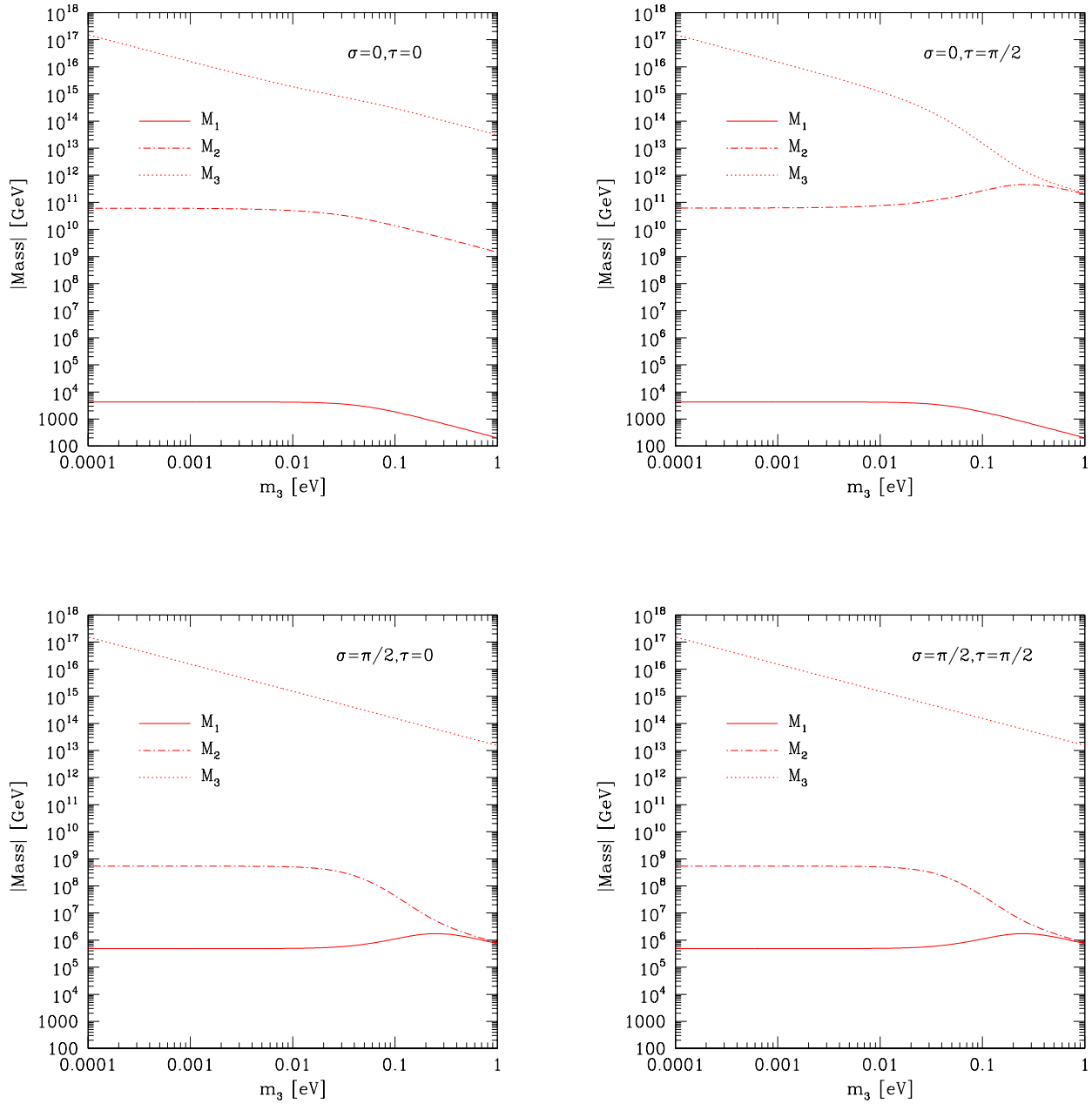


Figure 3: Same as Figure 2 for the inverted mass ordering.

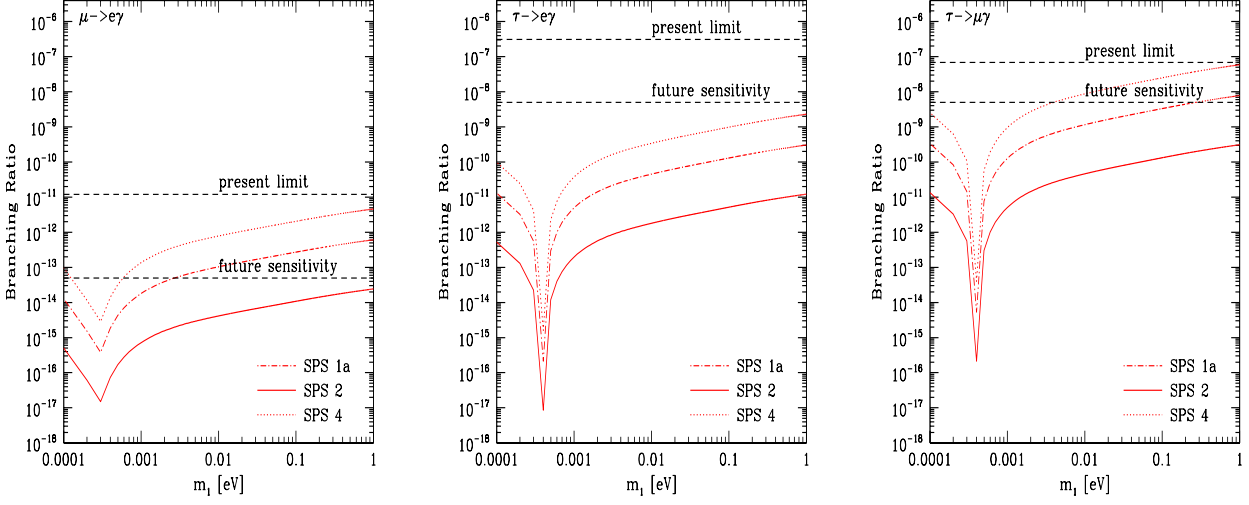


Figure 4: First realization of QLC: the branching ratios for $\mu \rightarrow e\gamma$, $\tau \rightarrow e\gamma$ and $\tau \rightarrow \mu\gamma$ against the smallest neutrino mass (normal ordering) for the SPS points 1a, 2 and 4, see Table 1. Indicated are also the present and future experimental sensitivities.

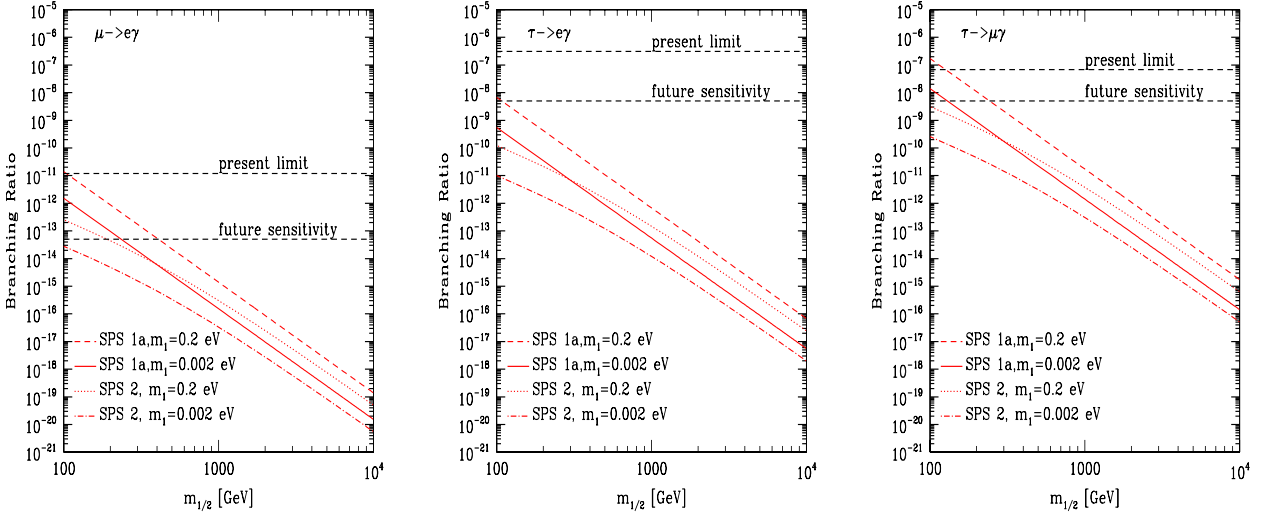


Figure 5: First realization of QLC: the branching ratios for $\mu \rightarrow e\gamma$, $\tau \rightarrow e\gamma$ and $\tau \rightarrow \mu\gamma$ against the SUSY parameter $m_{1/2}$ for the SPS slopes 1a and 2 see Table 1. We have chosen two values for the neutrino masses (normal ordering), namely 0.002 eV and 0.2 eV. Indicated are also the present and future experimental sensitivities.

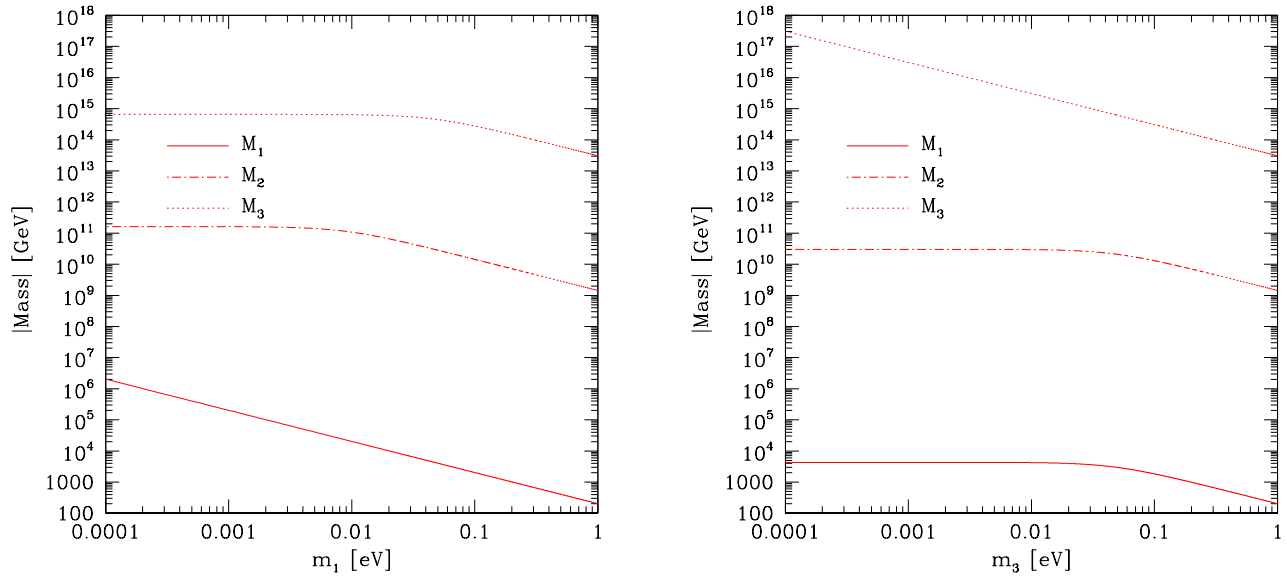


Figure 6: Second realization of QLC: the heavy neutrino masses as a function of the smallest neutrino mass for the normal (left plot) and inverted (right plot) mass ordering.

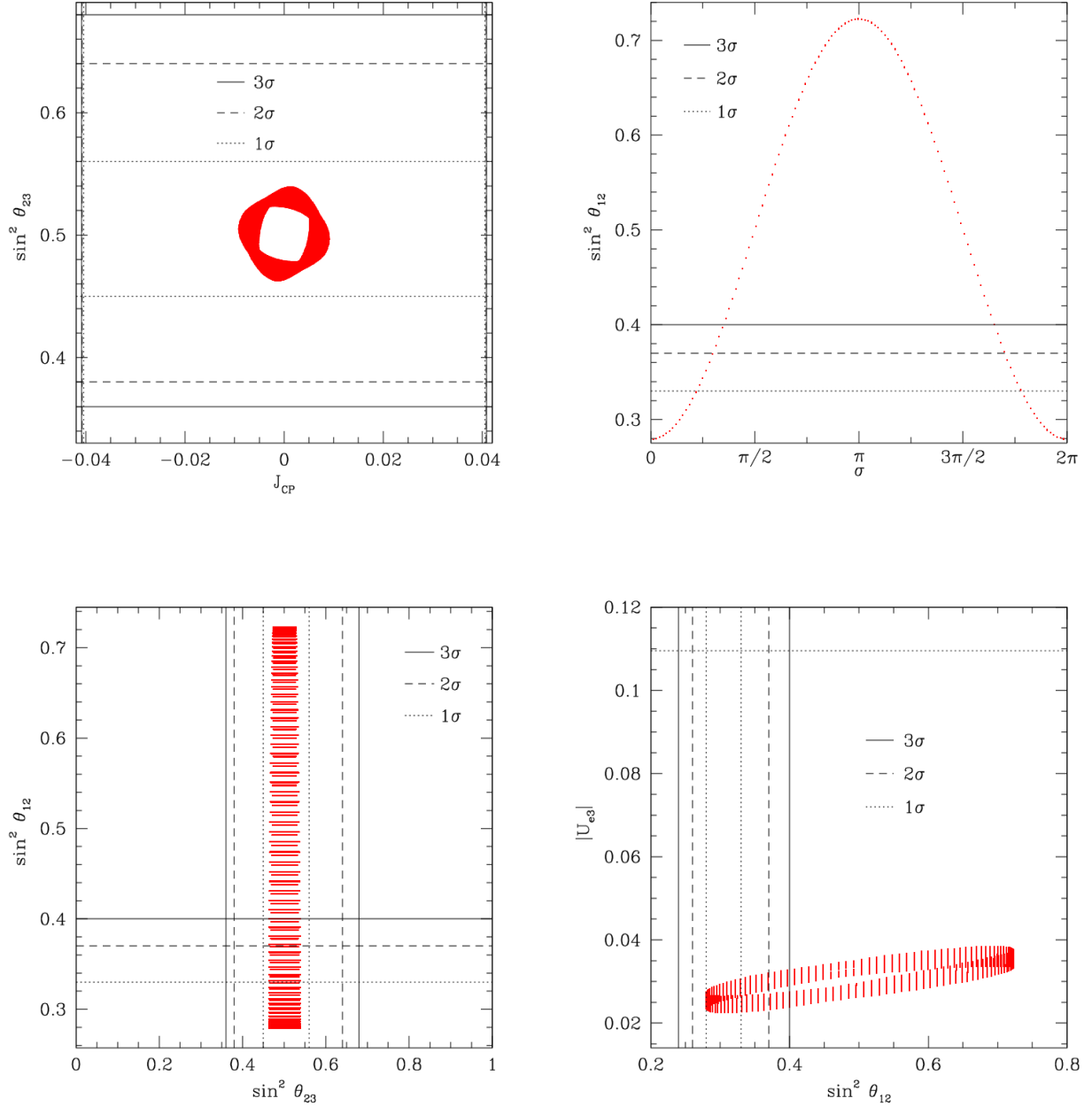


Figure 7: Second realization of QLC: neutrino observables resulting from Eq. (43) for the 3σ ranges of the CKM parameters. We also indicated the current 1, 2 and 3σ ranges of the oscillation parameters.

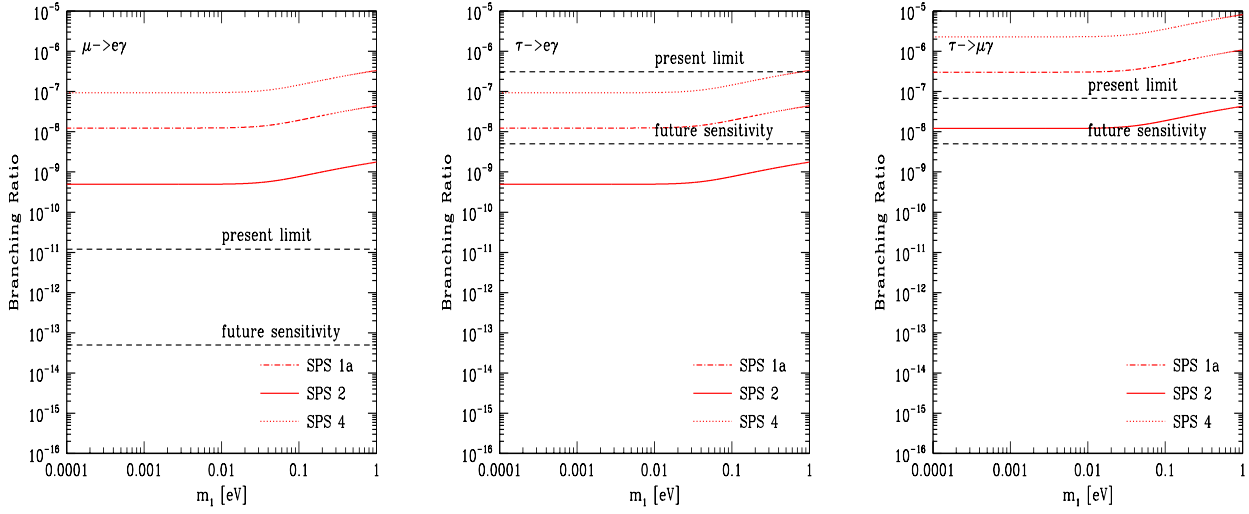


Figure 8: Second realization of QLC: the branching ratios for $\mu \rightarrow e\gamma$, $\tau \rightarrow e\gamma$ and $\tau \rightarrow \mu\gamma$ against the smallest neutrino mass (normal ordering) for the SPS points 1a, 2 and 4, see Table 1. Indicated are also the present and future sensitivities.

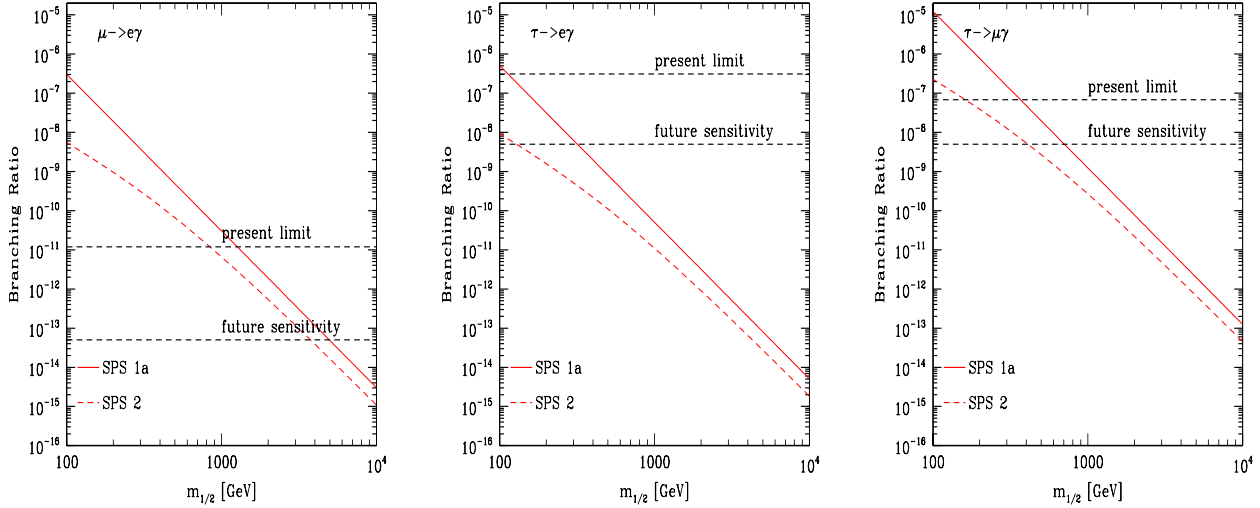


Figure 9: Second realization of QLC: the branching ratios for $\mu \rightarrow e\gamma$, $\tau \rightarrow e\gamma$ and $\tau \rightarrow \mu\gamma$ against the SUSY parameter $m_{1/2}$ for the SPS slopes 1a and 2, see Table 1. We have chosen for the neutrino mass (normal ordering) 0.02 eV. Indicated are also the present and future sensitivities.